

# SU2: a reliable computational framework for Non-Ideal Compressible Fluid Dynamics applications

G. Gori<sup>a,c</sup>, M. Zocca<sup>a,c</sup>, G. Cammi<sup>b,c</sup>, A. Spinelli<sup>b,c</sup>, P. M. Congedo<sup>d</sup>  
and A. Guardone<sup>a,c</sup>

Politecnico di Milano - Italy

<sup>a</sup> Department of Aerospace Science and Technology

<sup>b</sup> Energy Department

<sup>c</sup> CREA Lab

INRIA – France

<sup>d</sup> CARDAMOM Team



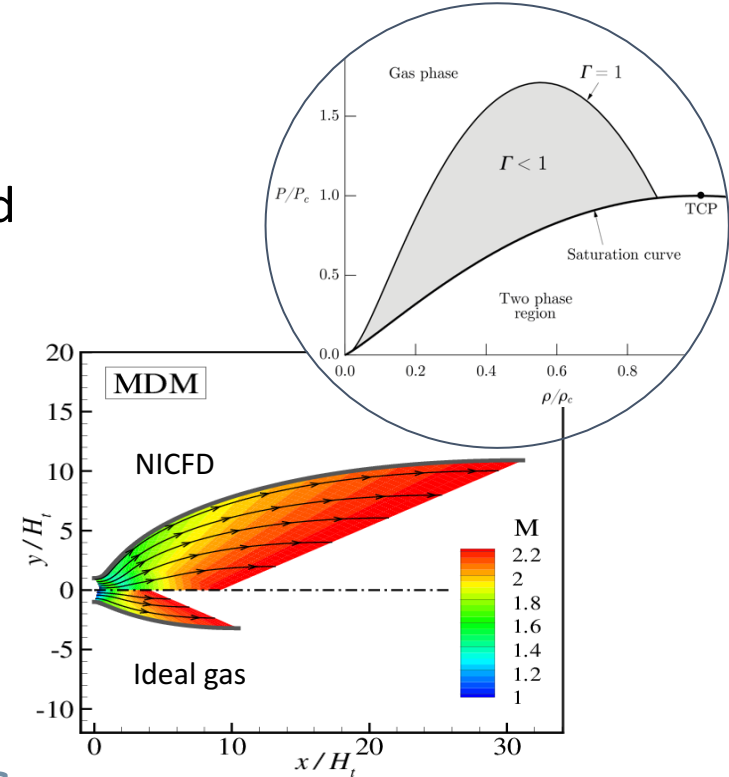
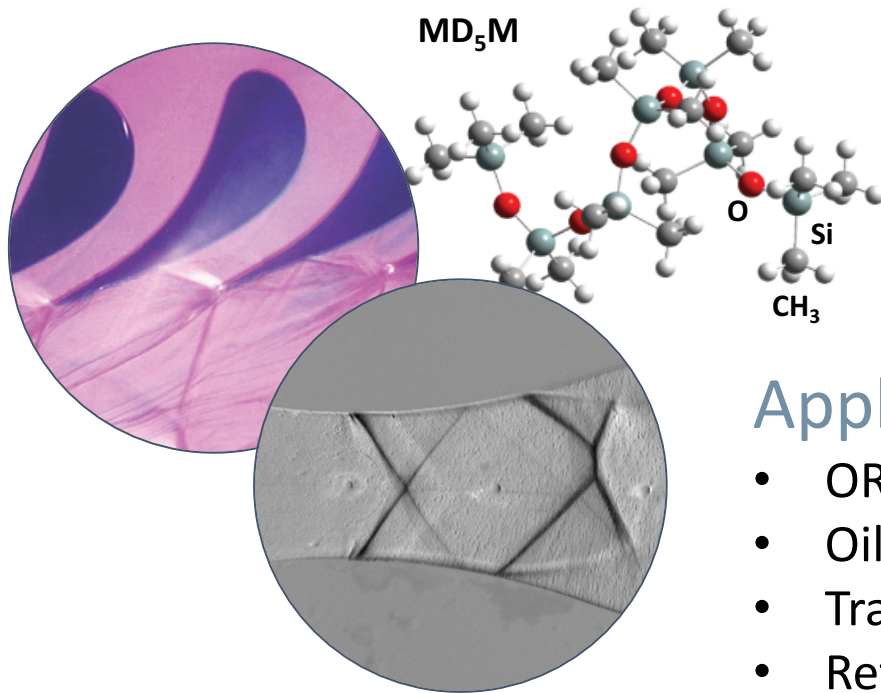
UTOPIÆ

Uncertainty  
Treatment and  
Optimisation in  
Aerospace  
Engineering

# Non-Ideal Compressible-Fluid Dynamics

## NICFD facts

- High compressibility effects
- Non-monotonic variation of the speed of sound
- Phase transition and TCP effects



## Applications

- ORC and SCO<sub>2</sub> plants
- Oil & Gas compression/expansion
- Trans-critical heat exchangers
- Refrigeration

...and many others!

None of currently available NICFD CFD codes was ever validated against experimental measurements in the NICFD regime

## OUTLINE

- SU2 NICFD solver validation
- Sliding mesh interface verification
- Future development



# The validation process: the framework

## Steps to validate the numerical NICFD solver against experimental data

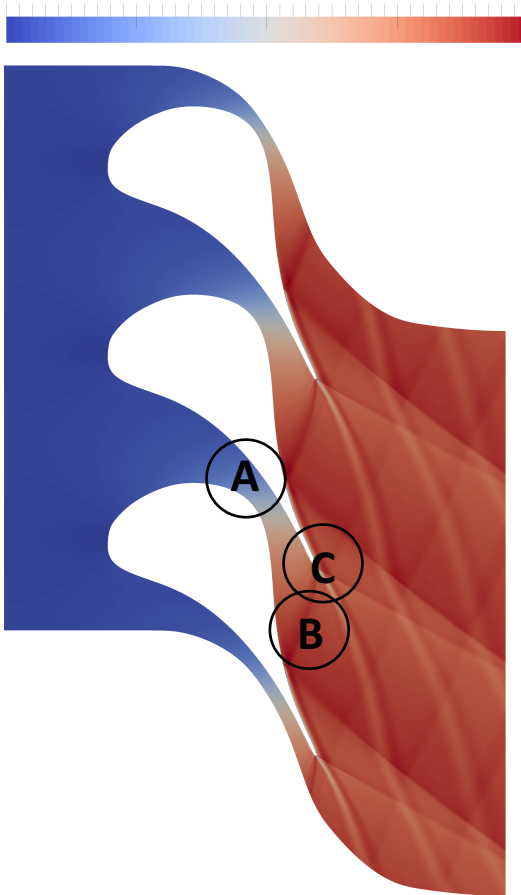
- Design simplified experimental benchmark tests
- Running CFD simulations using SU2 with different thermodynamic models
- Make numerical results grid independent using in-house mesh adaptation algorithm
- Carry out Uncertainty Quantification analysis using RobUQ, from INRIA, to assess CFD results against experimental data

The validation of the SU2 NICFD solver was presented @ ORC2017, Milano, Italy

# The validation process: test cases

## Mach

0 0,56 1,1 1,7 2,23



We identified 3 characteristic flow configurations that are representative of ORC applications:

A. Converging-diverging nozzle

B. Oblique shockwave and shock-boundary-layer interaction

C. Fishtail shock pattern at the blade trailing edge

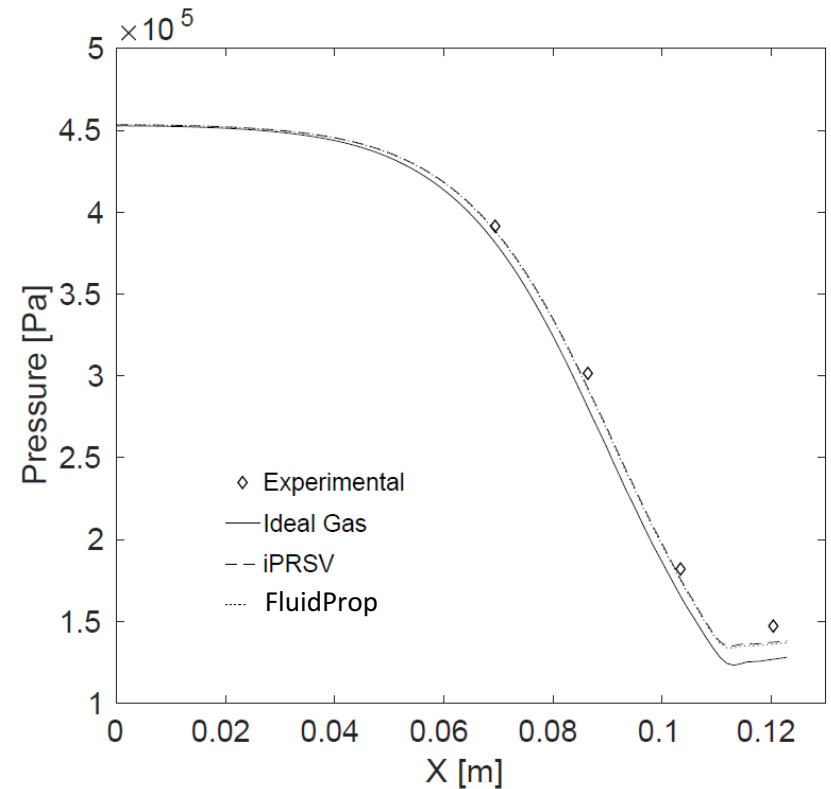
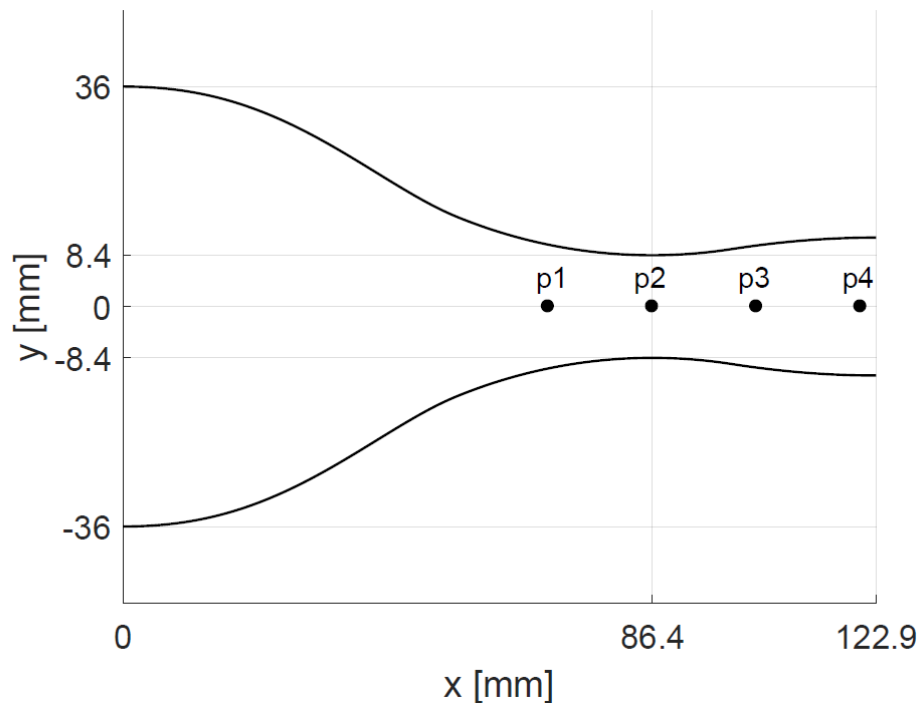
We designed 3 different test cases to validate the NICFD CFD solver

Pressure and temperature measurements, as well as schlieren images, were obtained from the TROVA test rig.

# Test case A: Non-Ideal supersonic expanding flow

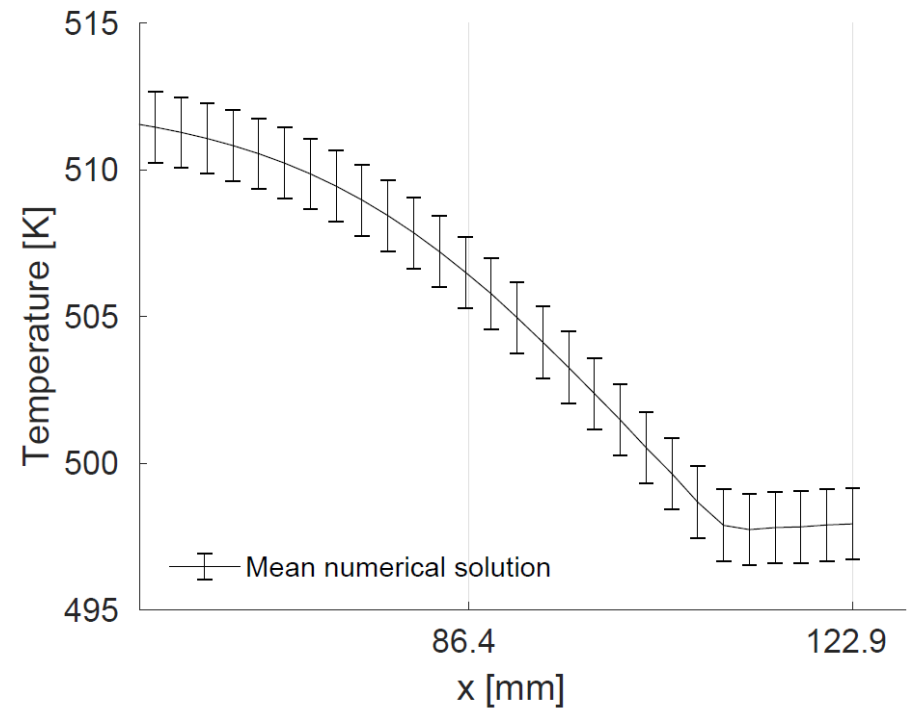
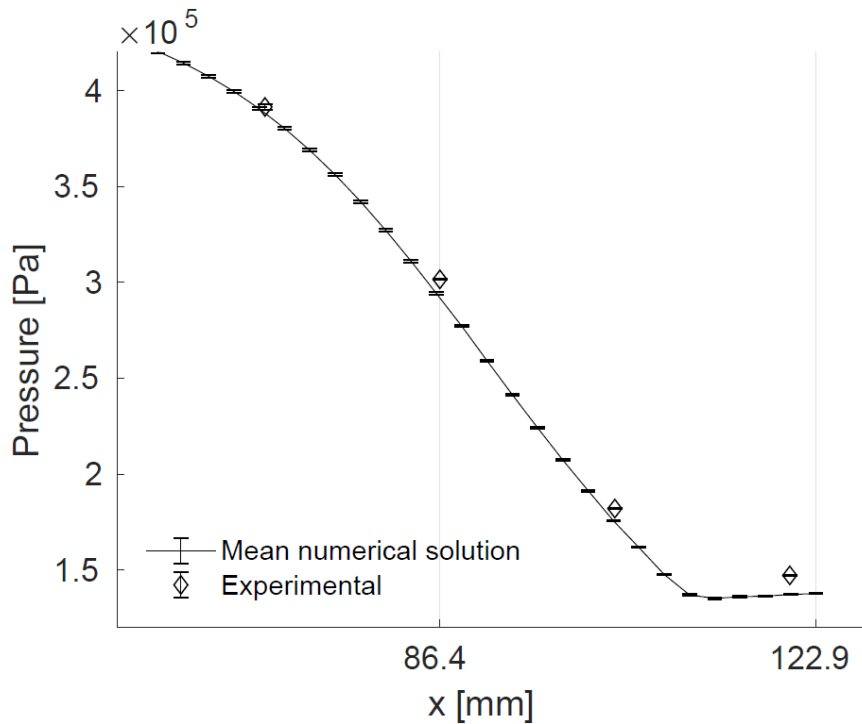
Fluid	Total $T / T_c$	Total $P / P_c$	Z
MDM	0.9	0.32	0.81

The flow was reproduced using three different equation of state, to evaluate the role of the thermodynamic model on the predicted solution



# Test case A: Non-Ideal supersonic expanding flow

Results from the uncertainty quantification analysis on the numerical solution

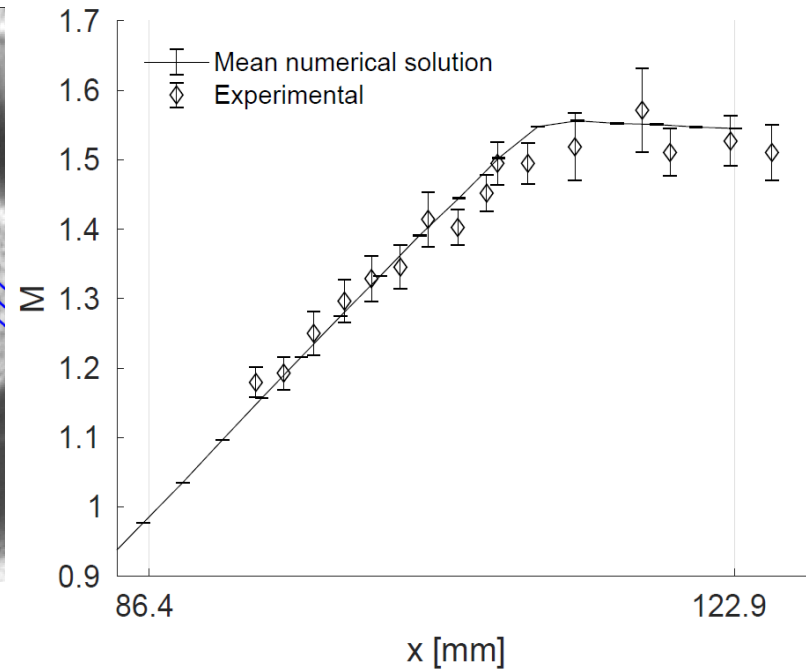
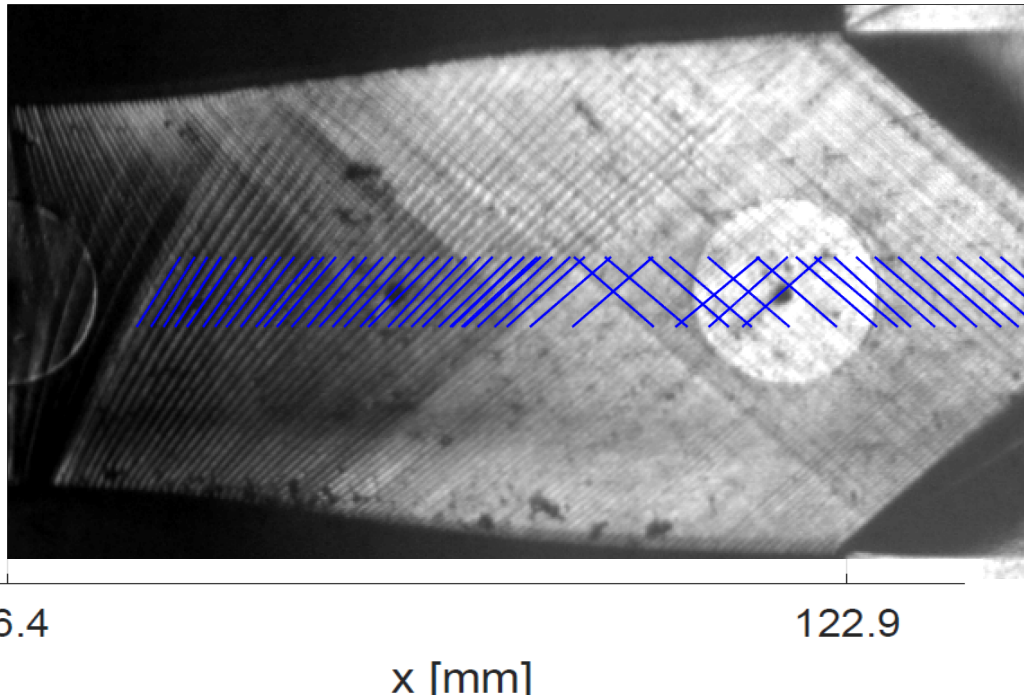


Very good agreement w.r.t. experimental data which proves robust and predictive solution

Robust prediction of the temperature (unc. < 0.2%)

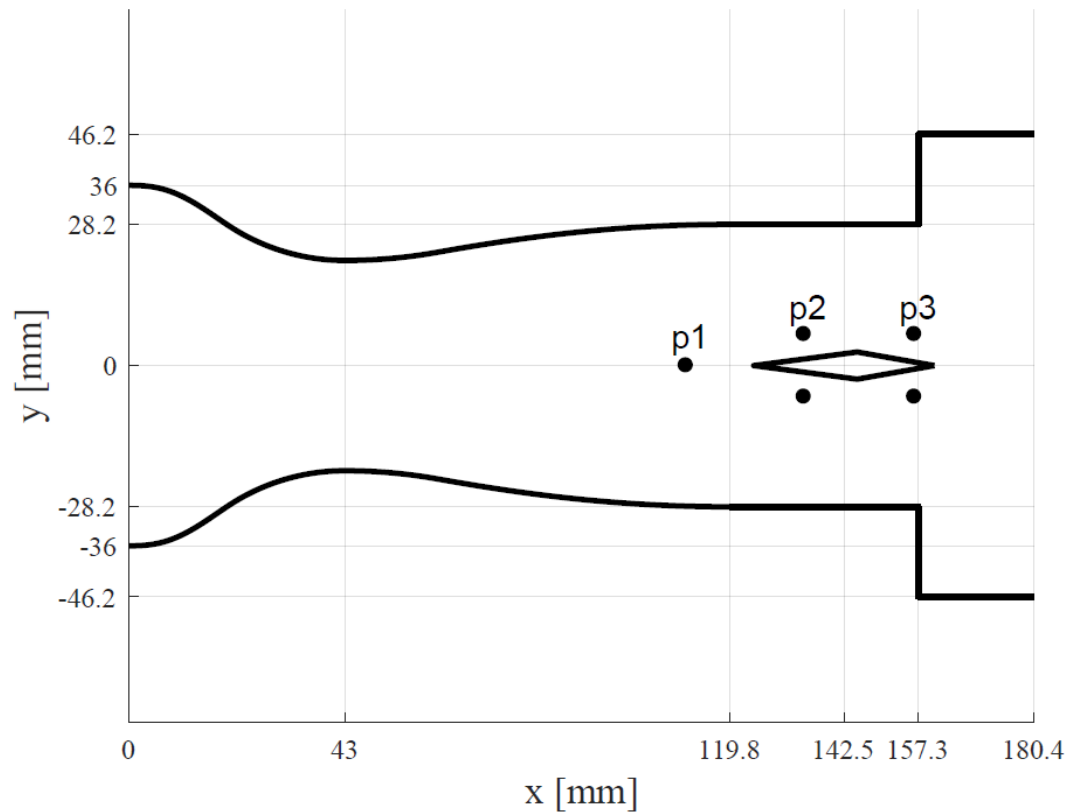
# Test case A: Non-Ideal supersonic expanding flow

The Mach number along the nozzle axis was measured from experimental schlieren images.



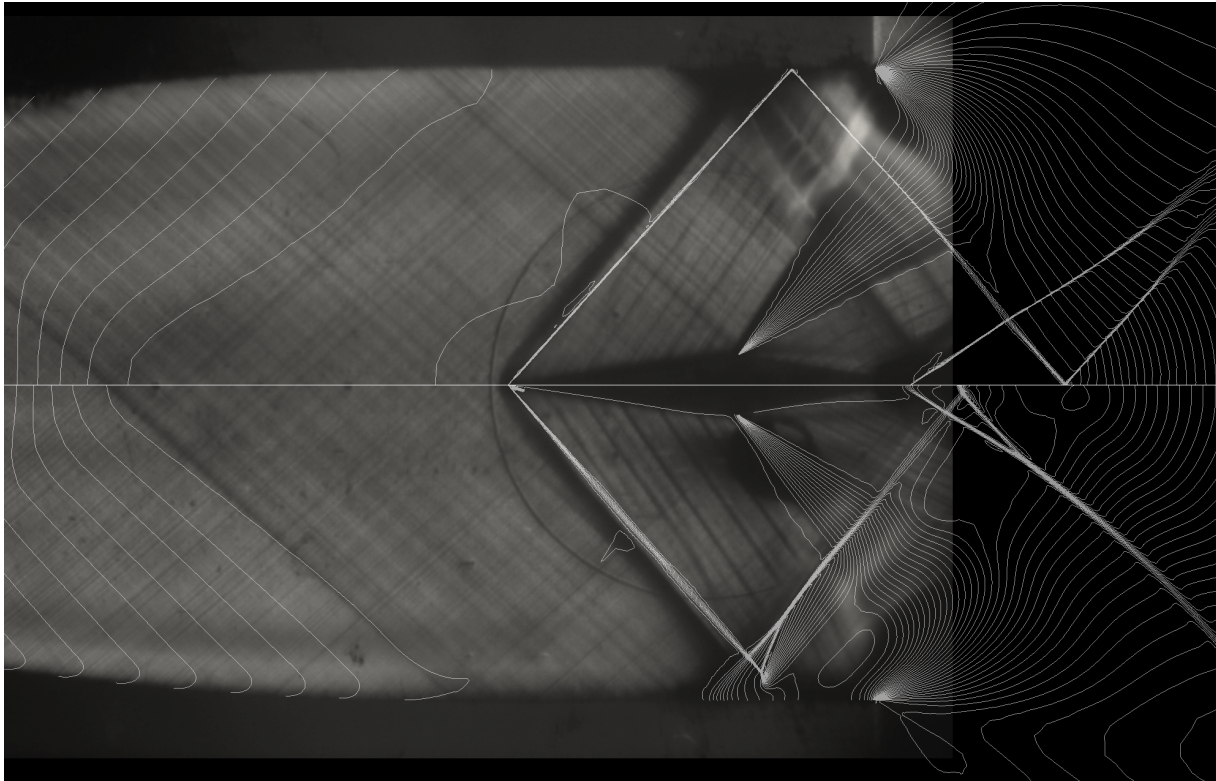
# Test case B: supersonic diamond-shaped airfoil

Fluid	Total $T / T_c$	Total $P / P_c$	Z
MDM	0.98	0.62	0.7



Ahead of the airfoil, the flow is approximately uniform at Mach 1.5 and Z 0.9.

# Test case B: supersonic diamond-shaped airfoil



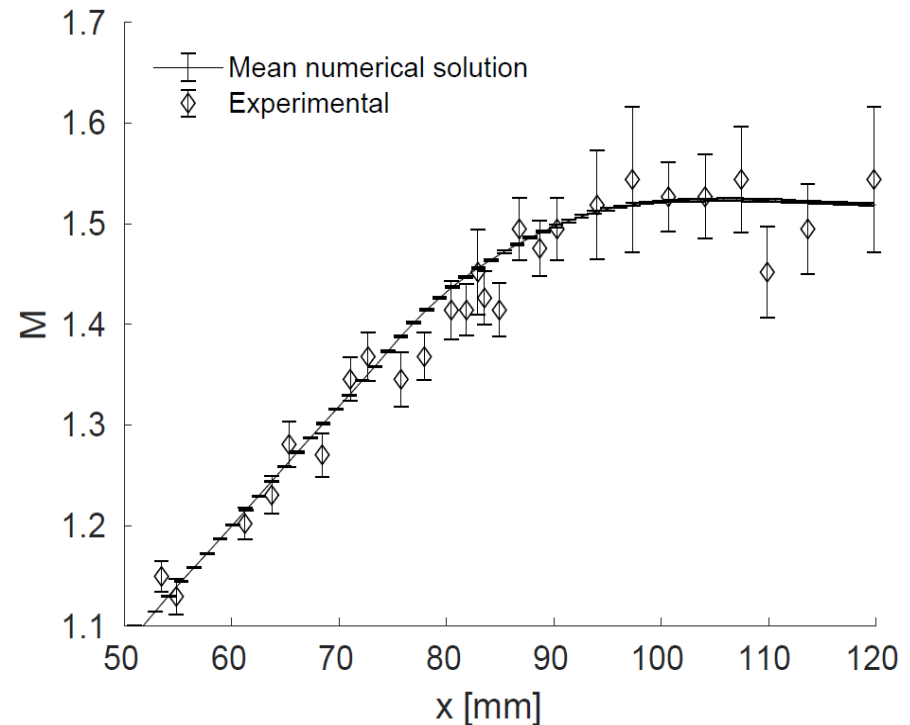
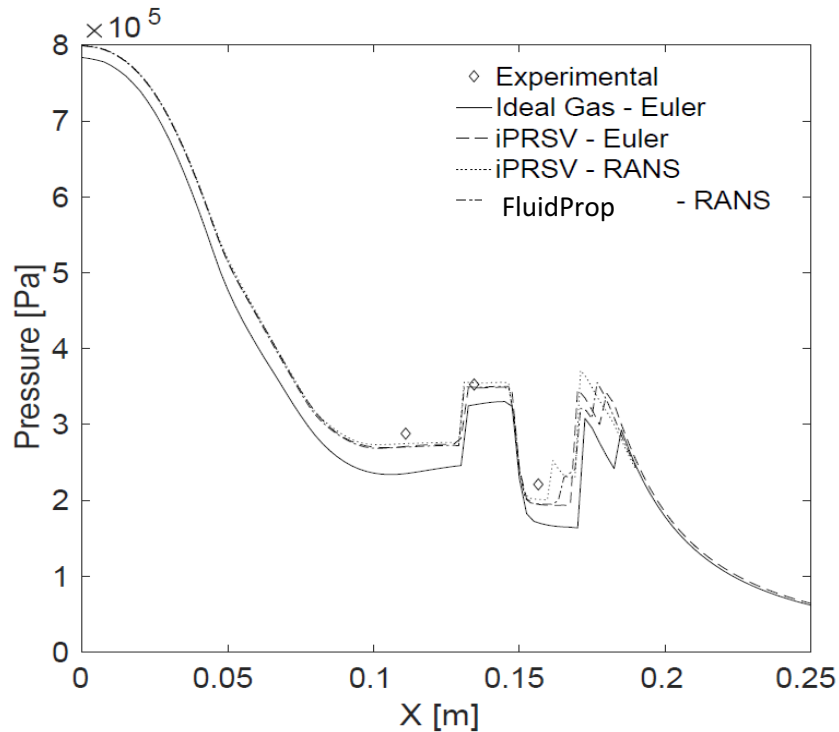
Euler (inviscid)

RANS (viscous)  
Spalart-Allmaras

The numerical solution includes a shock pattern that matches the one revealed by the experimental schlieren image.

# Test case B: supersonic diamond-shaped airfoil

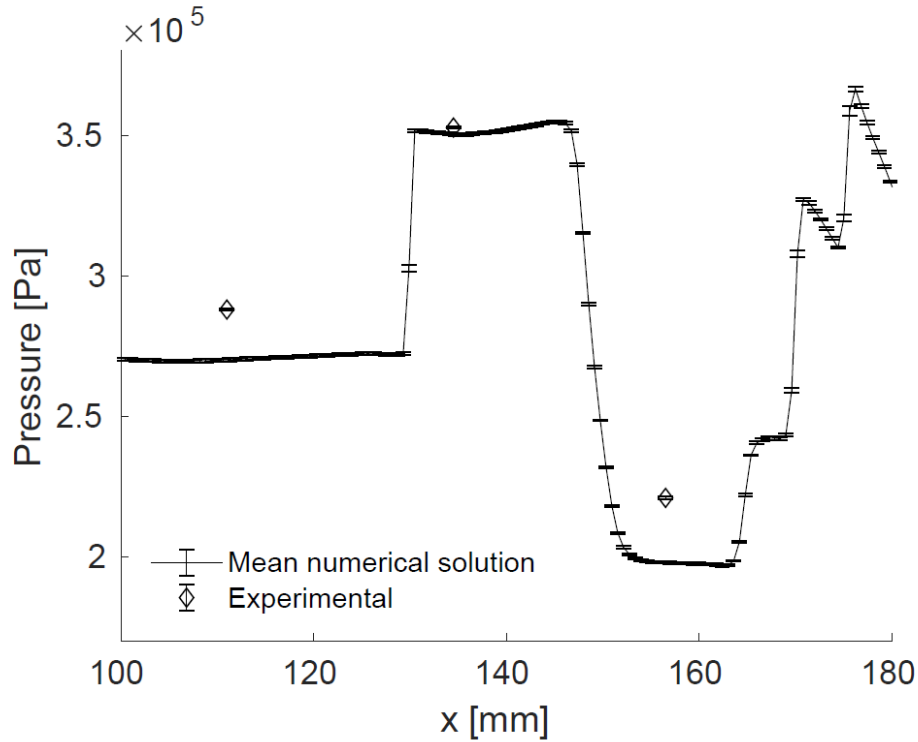
Up to 6 steps of grid adaptation process were enrolled, for both inviscid and viscid simulations. The quality of the solution was improved in the close proximity of shocks.



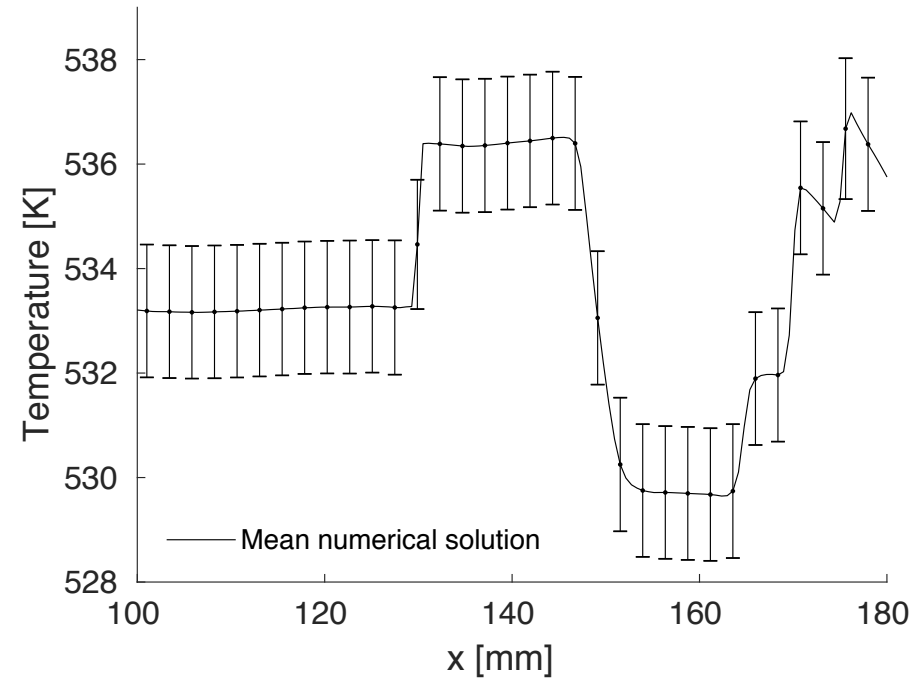
Numerical results are in good agreement with experimental data

# Test case B: supersonic diamond-shaped airfoil

Results from the uncertainty quantification analysis of the numerical solution



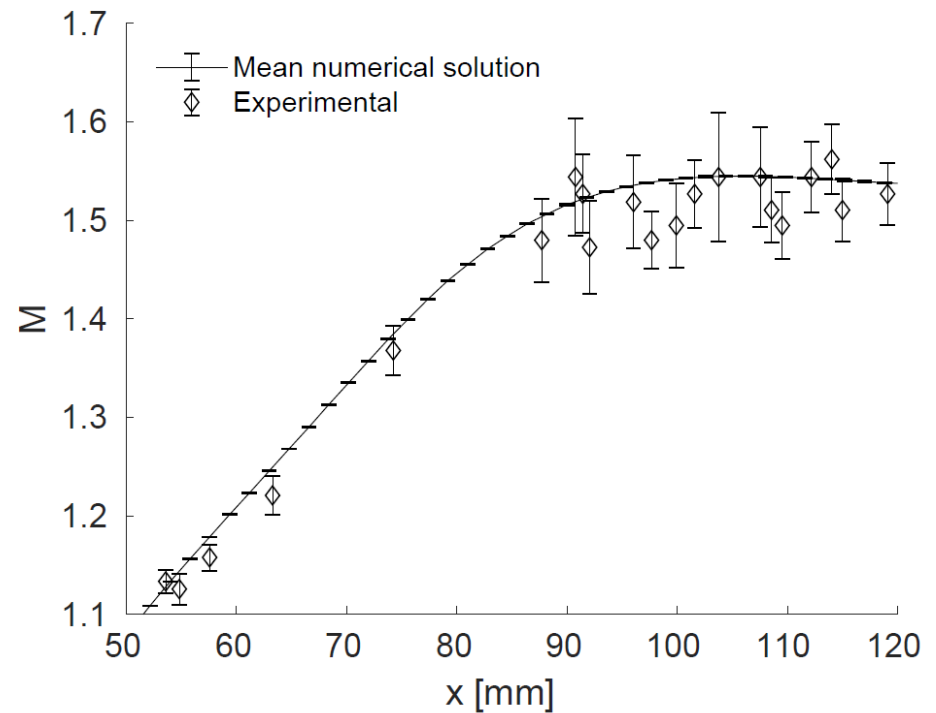
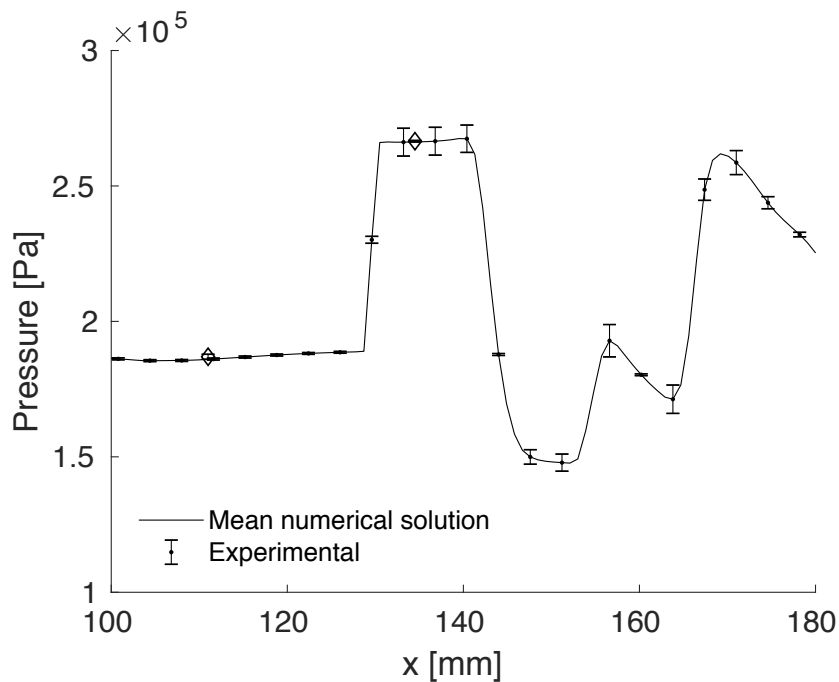
Maximal error of 12% with respect to the experiment



Robust prediction of the temperature (unc < 0.1%)

# Test case B: REVERSED supersonic diamond-shaped airfoil

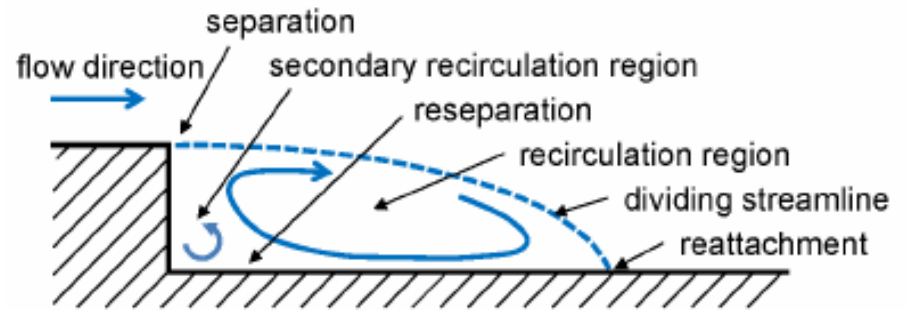
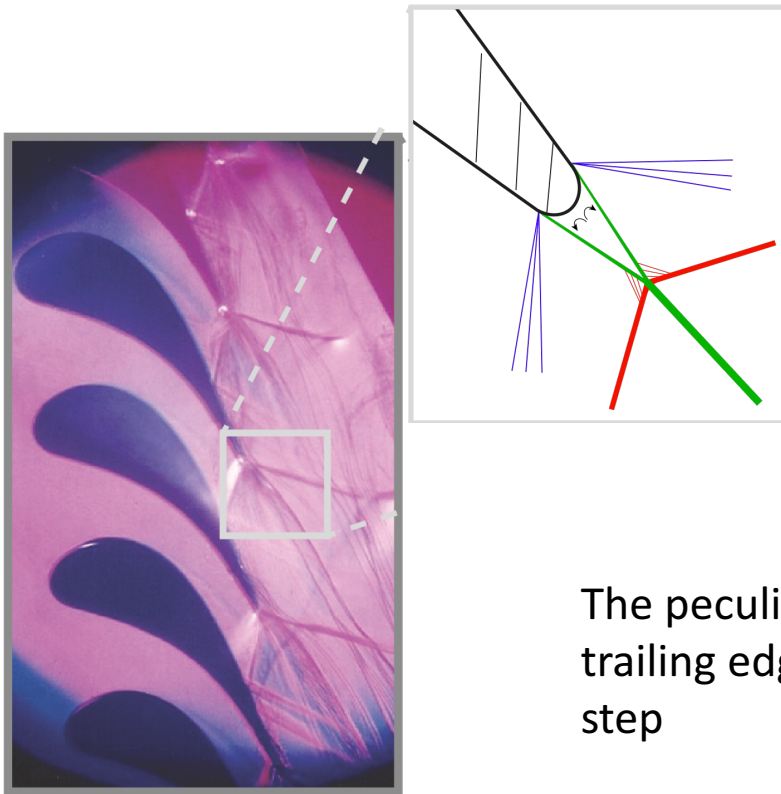
Fluid	Total $T / T_c$	Total $P / P_c$	Z
MDM	0.95	0.43	0.93



Uncertainty on the angle of attack of the airfoil was considered

# Test case C: backward facing step

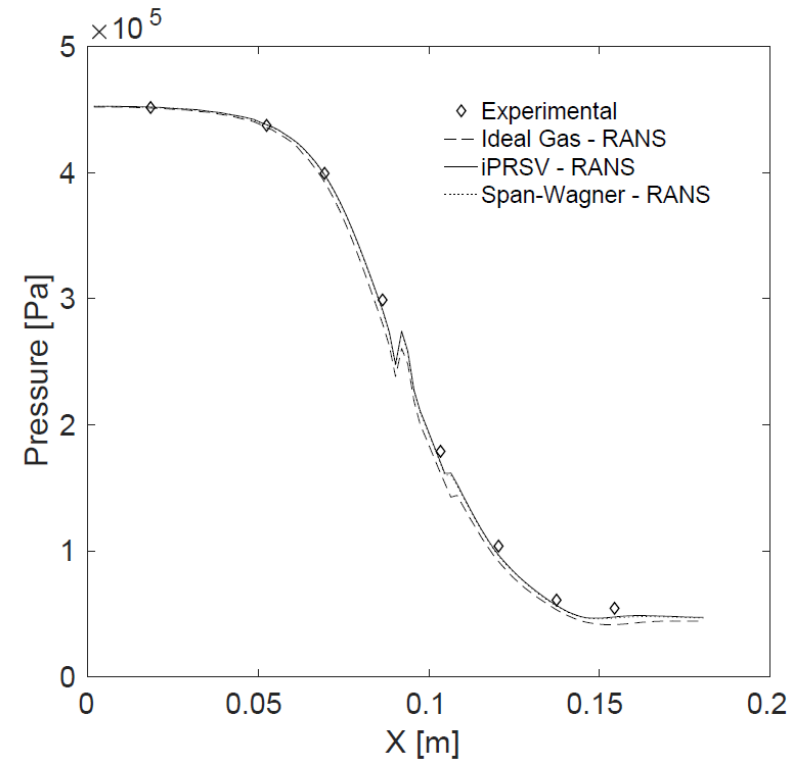
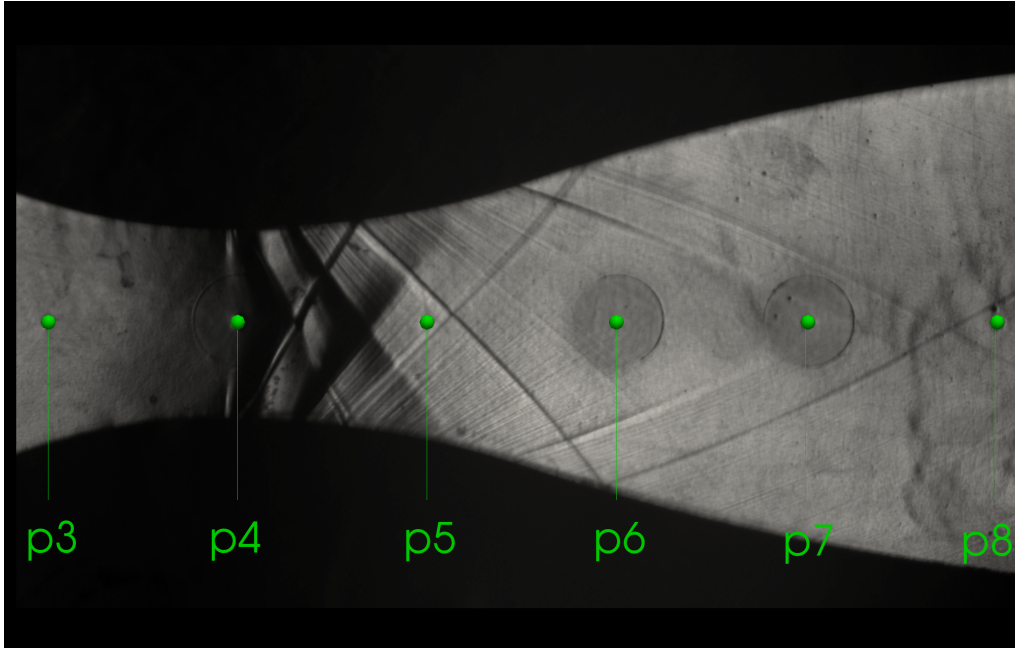
Fluid	Total T (reduced)	Total P (reduced)	Z
MDM	0.92	0.32	0.82



The peculiar flow configuration at the turbine blade trailing edge resembles the flow over a backward facing step

# Test case C: backward facing step

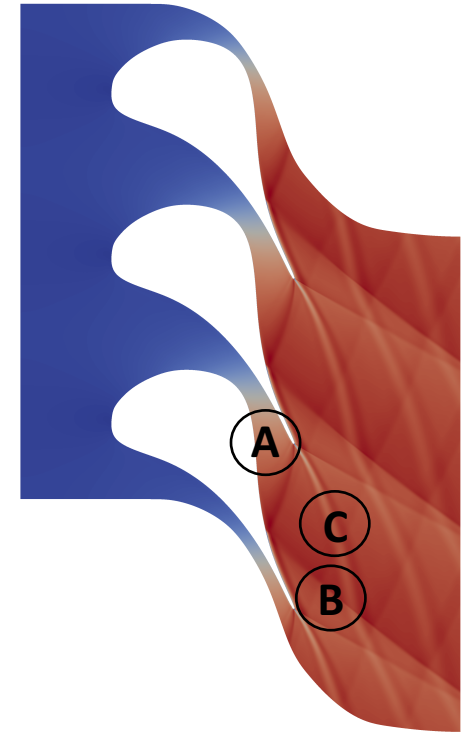
A small backward facing step is wrought, to set the nozzle throat.



Up to 3 steps of grid adaptation procedure were enrolled, for both inviscid and viscous simulations. The quality of the solution was improved in the close proximity of shocks.

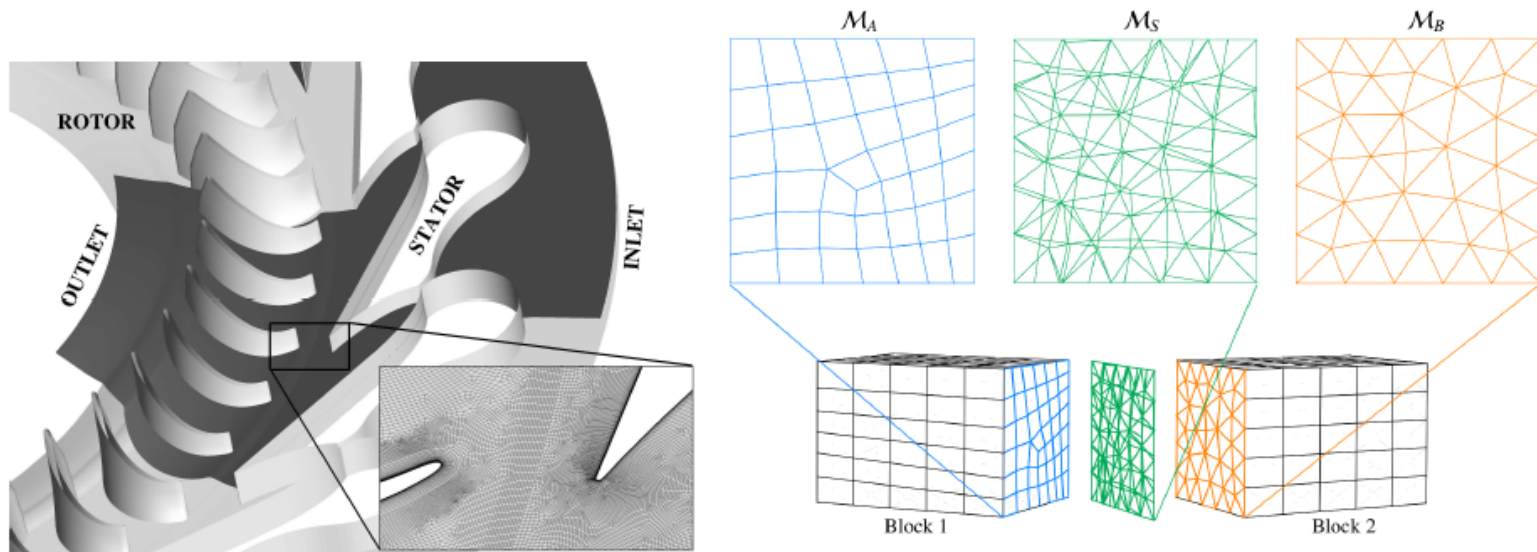
# Summarizing...

- For the first time, the capabilities of a Non-Ideal Computational Fluid Dynamics (NICFD) solver were assessed against experimental results regarding flows of fluid in a non-ideal regime.
- The NICFD CFD solver from the SU2 open-source suite proved to predict fairly accurate results, for a set of exemplary test cases of interest for ORC applications
- Uncertainty Quantification was carried out proving small error bars for the numerical solution, pressure (<0.01%) and temperature (0.2%).



Very robust and predictive numerical solution with respect to the experiments!

# Verification of the sliding mesh interface



<sup>1</sup> Models and Simulation of Non-Ideal Fluid Flows in Unconventional Turbomachinery Ph.D. Thesis 2015

There are two different sliding mesh approaches currently available in SU2

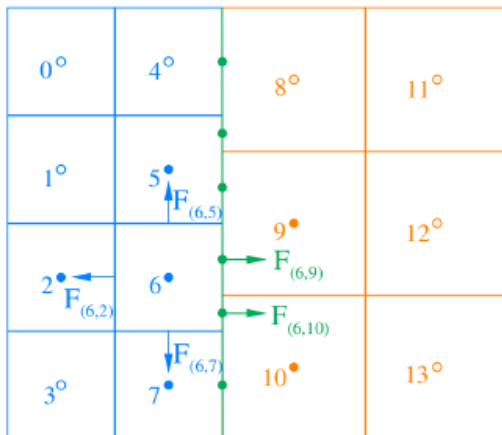
- The Nearest Neighbour approach NN
- A Weighted Averaged approach WA (E. Rinaldi<sup>1</sup>)

The verification of the SU2 sliding mesh interface was presented @ Coupled Problems 2017, Rhodes Island, Greece

# Sliding mesh implementation in SU2

A loosely coupled problem...

Governing equations are solved independently over each zone. In order to enforce the coupling between different zones, the sliding interface is assumed to act as a boundary onto which a non-uniform outer state is applied.



Given a domain  $\Omega$  and being  $\delta\Omega$  its surface boundary

$$\mathbf{U} = (\rho, \rho\mathbf{v}, E^t)^T$$

$$\frac{\partial}{\partial t} \int_{\Omega} \mathbf{U} d\Omega + \int_{\partial\Omega} \mathbf{F}(\mathbf{U}) dA = 0$$

$$\frac{\partial \mathbf{U}_k}{\partial t} = -\frac{1}{V_k} \left[ \sum_{p=1}^{N_{fi}} A_p \mathbf{F}(\mathbf{U}_k, \mathbf{U}_p) + \sum_{p=1}^{N_{fb}} A_p \left( \sum_{q=1}^{N_{sl}} W_q \mathbf{F}(\mathbf{U}_k, \mathbf{U}_q^{sl}) \right) \right]$$

# Sliding mesh implementation in SU2

NN: the boundary state at the interface is retrieved locally by taking the state of the nearest node from the other block

It is equivalent to a piecewise constant BC

- Conservation generally not guaranteed
- Consistent
- Quite cheap
- Low accuracy
- Requires a Nearest Neighbor search

$$N^{sl} = 1 \text{ and } W_1 = 1$$

WA: the numerical flux at the cell interface is retrieved locally by averaging the nominal fluxes towards each of the cells of the opposite block that share the same portion of the sliding interface.

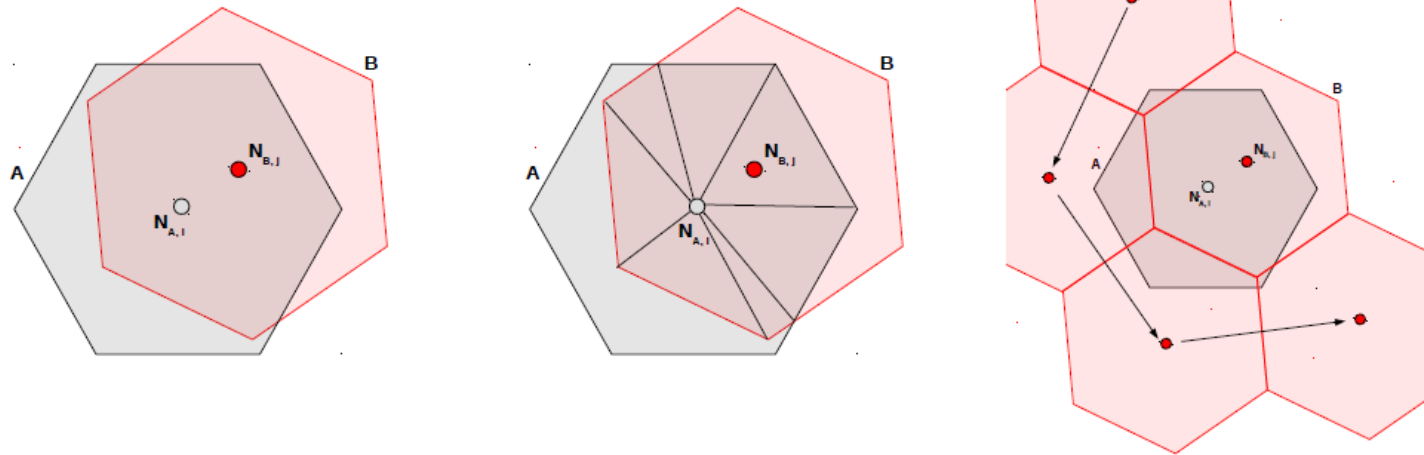
At the interface, the numerical flux is assembled by summing up all the nominal fluxes weighted by a geometrical scale factor

- Conservation generally not guaranteed
- Consistent
- Expensive
- Higher accuracy

$$N^{sl} = ? \text{ and } W_1 = ?$$

Requires the construction of an auxiliary data structure: the *supermesh*

# The “local” supermesh

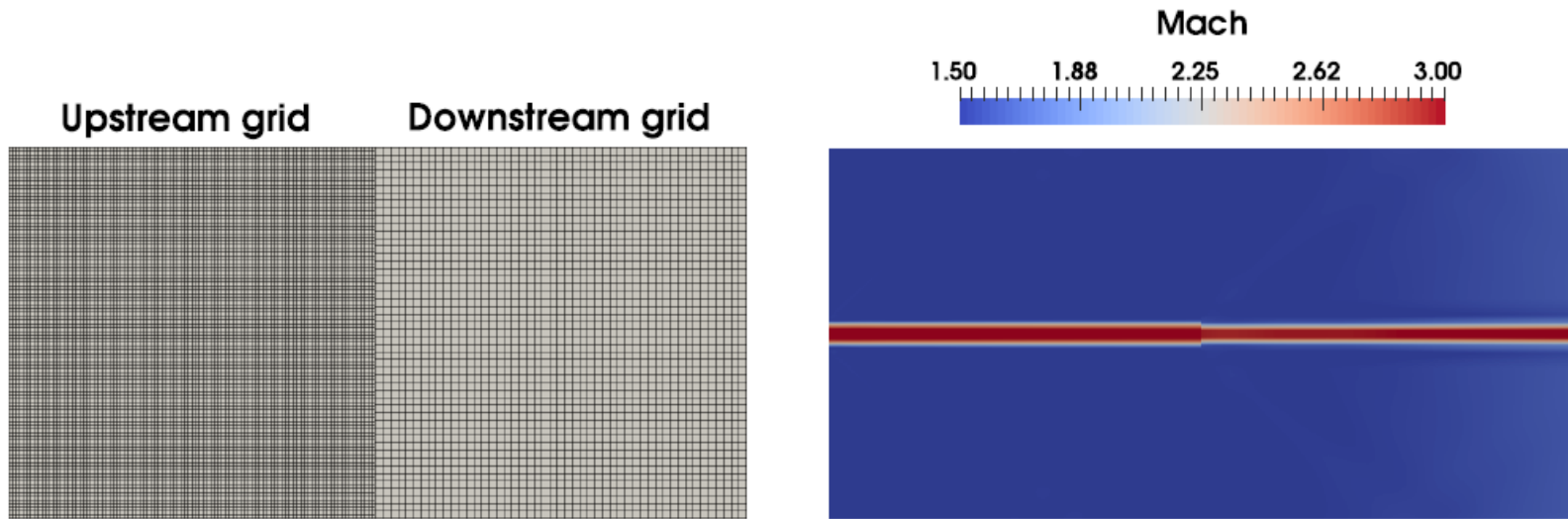


## Supermesh construction

1. Identify nodes of block B contained in A (NN search could be employed)
2. Compute intersection points among edges of A and B
3. Decompose the overlap region into triangles
4. Compute the overlap area (and the weight  $W_i$ ) for element  $B_i$

Repeat for each element of the layer of neighboring elements

# Verification of the sliding mesh interface: case A

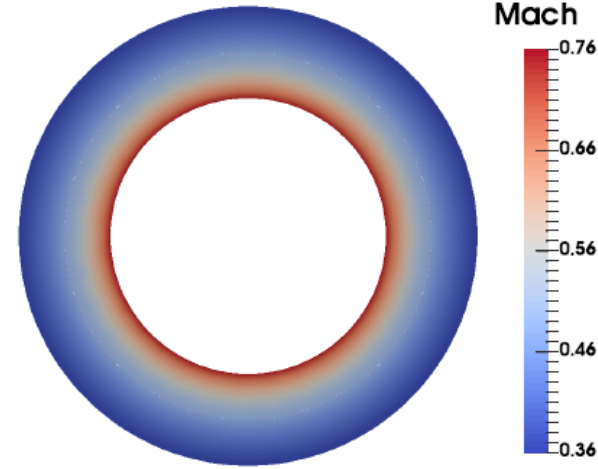
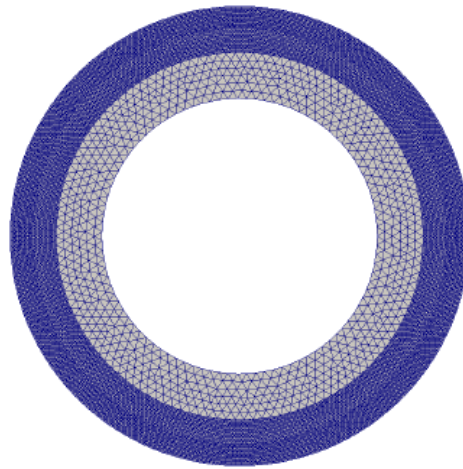


Steady supersonic Euler flow.  
Mean flow Mach number: 1.5  
Jet stream Mach number: 3.0

Nominal mass flow 620.7880 Kg/s

$\Delta h_2$	$10\Delta h_1$	$5\Delta h_1$	$\Delta h_1$	$0.1\Delta h_1$
NN	589.9025	614.5973	620.7225	620.4261
WA	620.7192	620.7212	620.7225	620.7062

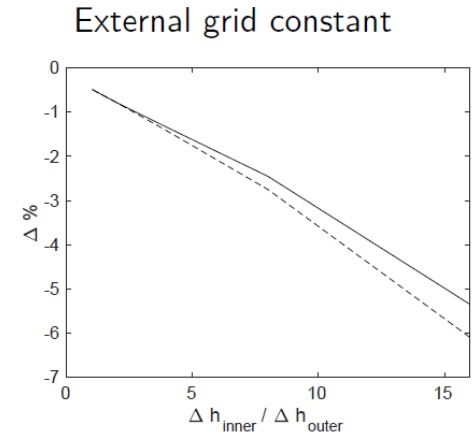
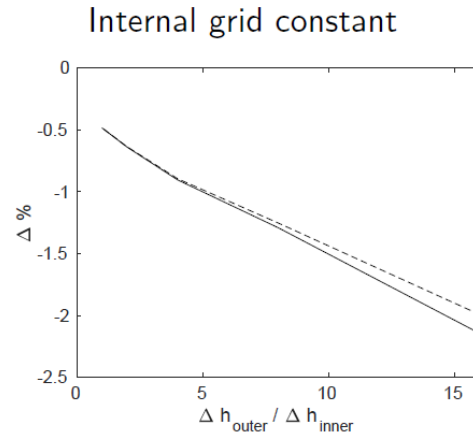
# Verification of the sliding mesh interface: case B



Flow sink: steady axisymmetric Euler flow. Differential pressure applied at the boundaries

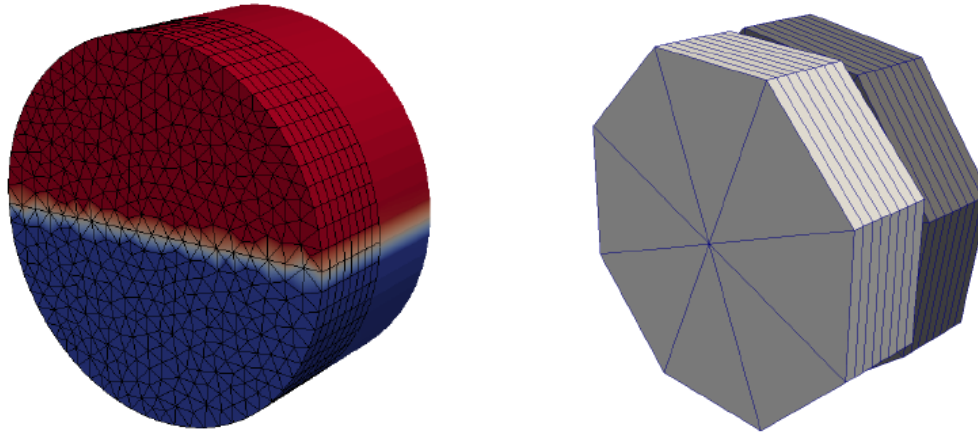
For conformal grids, the NN and the WA approach has an equivalent behaviour

$\Delta h$	0.8	0.4	0.2	0.1	0.05
$\Delta\%$	-7.55	-3.50	-1.84	-0.95	-0.48

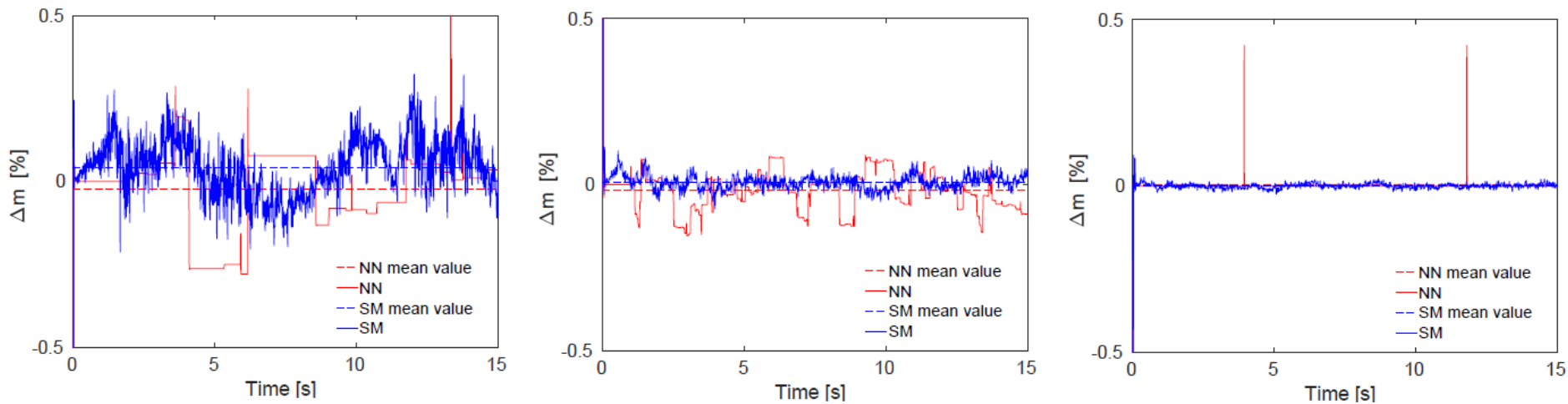


NN (continuous line) and WA (dashed line)

# Verification of the sliding mesh interface: case C



Steady Euler flow. Upper Mach number: 3.0. Lower Mach number: 1.5.



Conservation was assessed for 3 different level of grid resolution.

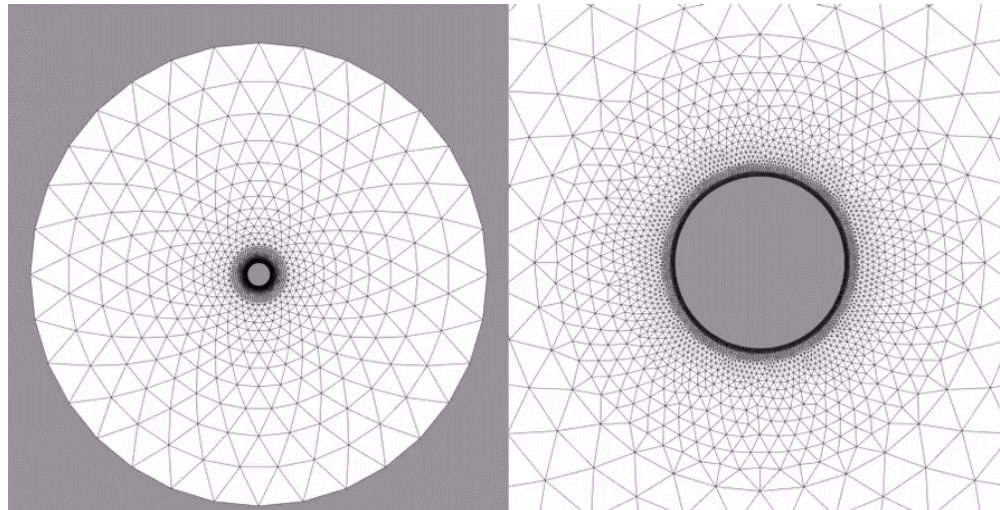
# We are not satisfied yet...

We are working on a locally adaptive sliding mesh approach!  
We aim at designing a robust, fully conservative, method!

Nodes are added to both zones to produce conformal boundaries over the sliding interface.



1. Pre-processing step: nodes from boundary A are added to B, and viceversa
2. Pre-processing step: grid elements over the interface are split
3. As the two grids slide, edges are swapped to maintain conformity



# Ongoing work...

- Local adaptive sliding mesh approach (turbomachinery applications, wind turbines...)
- Design new experiments to explore more thoroughly the NICFD region and extend the SU2 NICFD solver validation (different fluids, geometries...)
- Uncoupled Particle Tracking solver to reconstruct the trajectories of dispersed particles (to simulate LDV, sprays...)

...questions?

# Thanks for your attention!



The research is funded by the European Research Council under Grant ERC Consolidator 2013, project NSHOCK 617603



**European Research Council**  
Established by the European Commission

# The validation process: Uncertainty Quantification

## The role of Uncertainty Quantification

Multiple (physical and modelling) sources of uncertainty exists!

The main goal of the Uncertainty Quantification is to take into account system uncertainties (parameters, measurements, model etc) in order to quantify the statistical variability of a quantity of interest.

We will focus on the propagation of experimental uncertainties through the CFD code to compare numerical and experimental error bars.

Need for an efficient stochastic method to propagate uncertainty



# The validation process: setting up the UQ framework

## Coupling SU2 with a non-intrusive library, RobUQ from INRIA

RobUQ includes innovative methods for solving forward and inverse UQ problems and optimization under uncertainties problems.

- A Polynomial-Chaos based method is used
- Based on the state-of-the-art papers<sup>1</sup>, we will only consider uncertainties on the initial conditions
- Uncertainties on the thermodynamic model are neglected with respect of other sources of uncertainty<sup>2</sup>
- Considered uncertainties are on the initial value of pressure and temperature

<sup>1</sup> P.M. Congedo, C. Corre, P. Colonna, J. Witteveen, G. Iaccarino, *Backward uncertainty propagation method in flow problems: application to the prediction of rarefaction shock-waves*, **Comput. Methods Appl. Mech. Engrg** 2012, Volume 213-216, Issue:1, pp.314-326.

<sup>2</sup> P. Cinnella, P.M. Congedo, V. Pediroda, L. Parussini, *Quantification of Thermodynamic Uncertainties in Real Gas Flows*, **International Journal of Engineering Systems Modelling and Simulation**, Vol. 2, Nos ½, 2010, pp 12-24

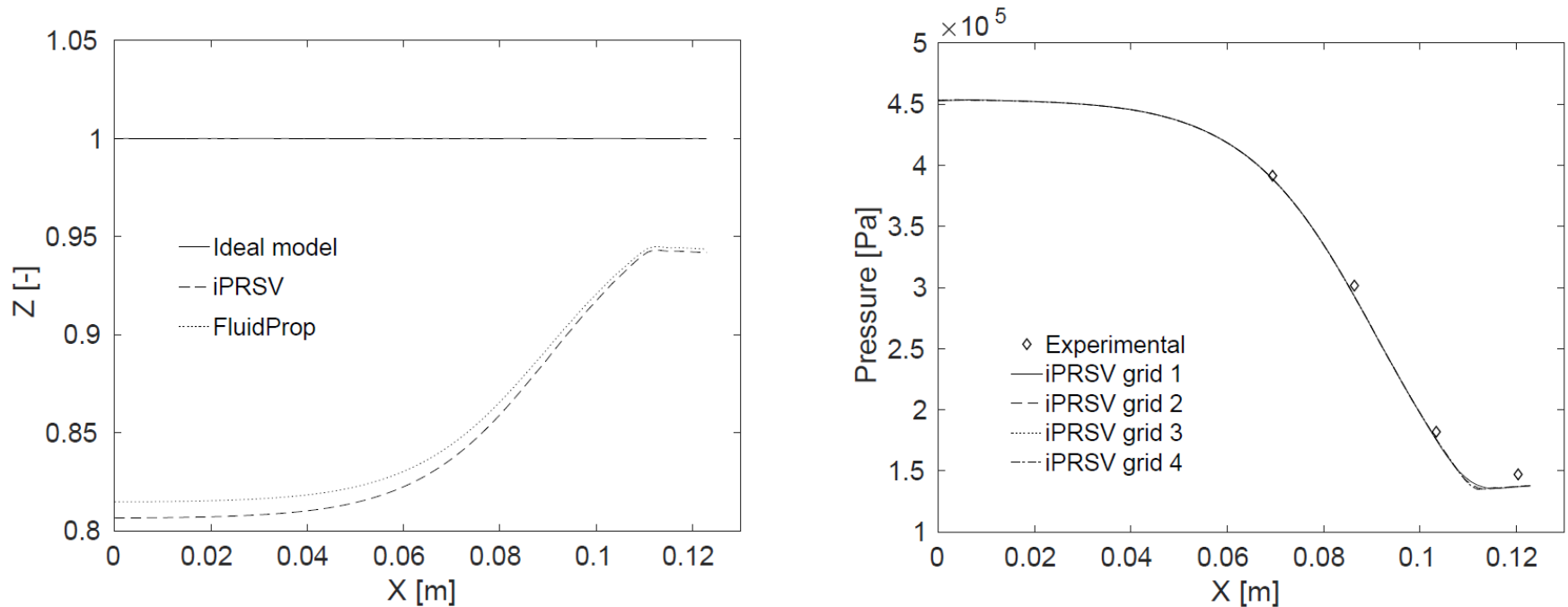
# Computational framework: why SU2?

- **An open-source model:** basic formulation with a reasonable set of initial capabilities
- **Portability:** SU2 has been developed using ANSI c++ and only relies on widely available, well supported, open-source software
- **Flexibility:** required to re-purpose existing software for new and different uses. Reusability and encapsulation enabling a common interface for all the necessary components.
- **Gradient availability:** for many applications it is important to obtain grad of the responses computed by SU2 to variations of design parameters

New capabilities are continuously added by an international team of developers spread all over the world: fluid models, turbomachinery design, grid adaptation, sliding meshes and many others...

# Test case A: Non-Ideal supersonic flow

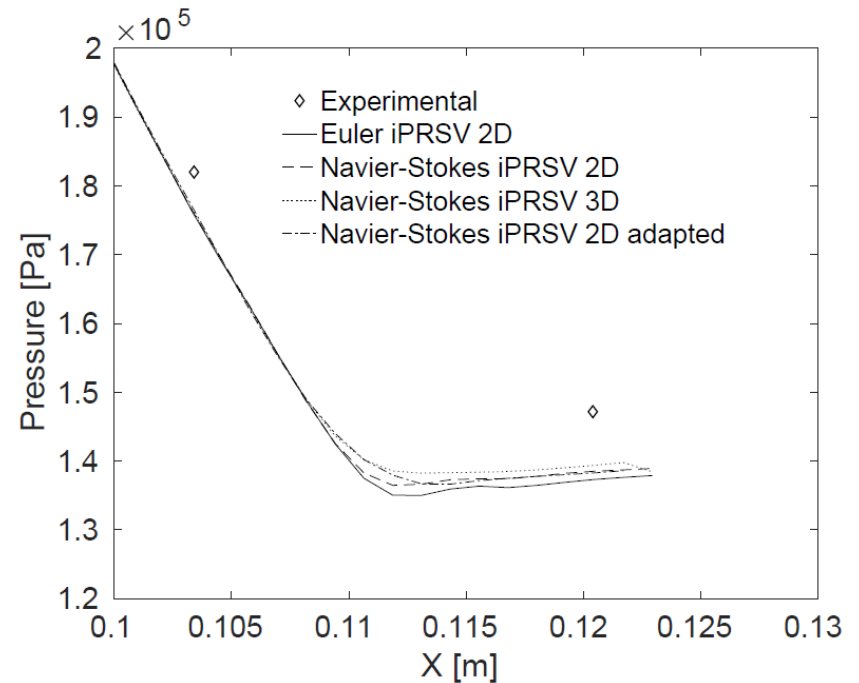
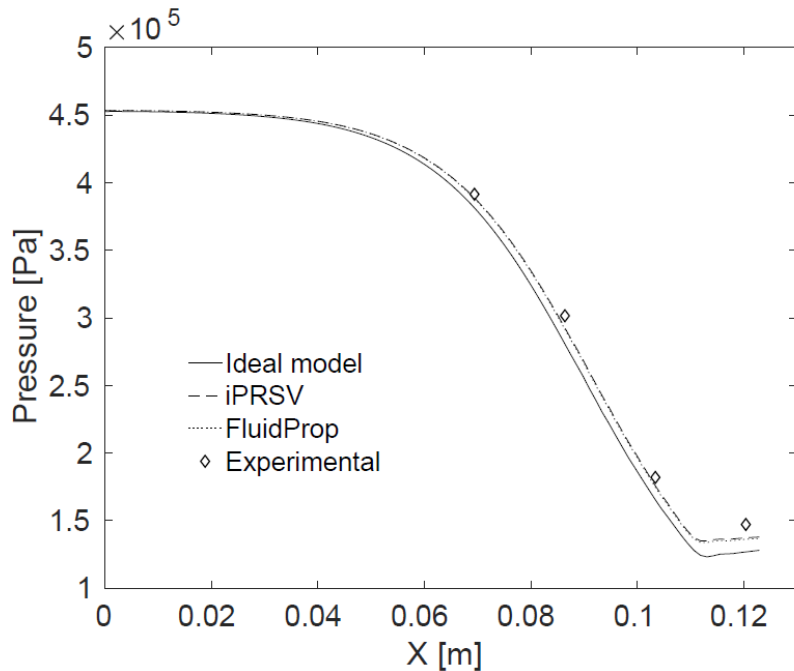
Grids with a different level of resolution to assess the dependency of the solution from the spatial discretization (300 to 15000 grid points), for inviscid simulations



The pressure trend reconstructed numerically fairly matches experimental measurements!

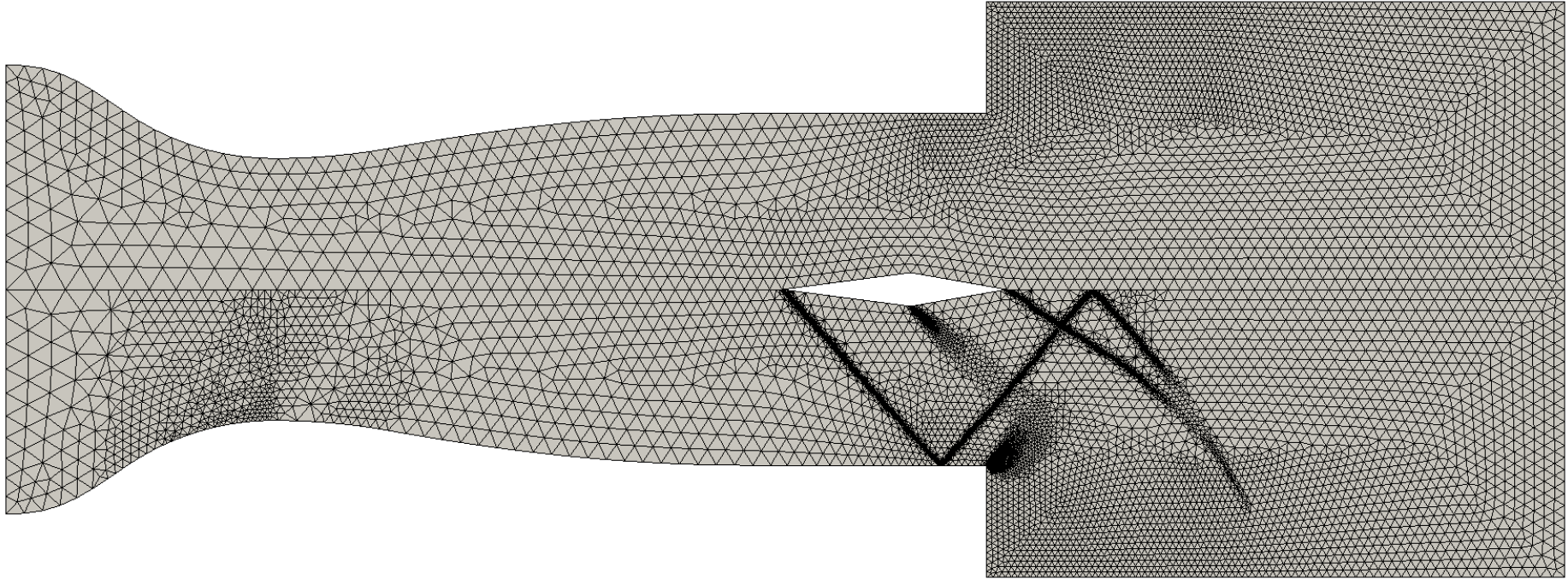
# Test case A: Non-Ideal supersonic flow

The very same test case was reproduced exploiting state-of-the-art EoS (the Helmholtz EoS embedded in the FluidProp library) and relaxing the inviscid assumption.



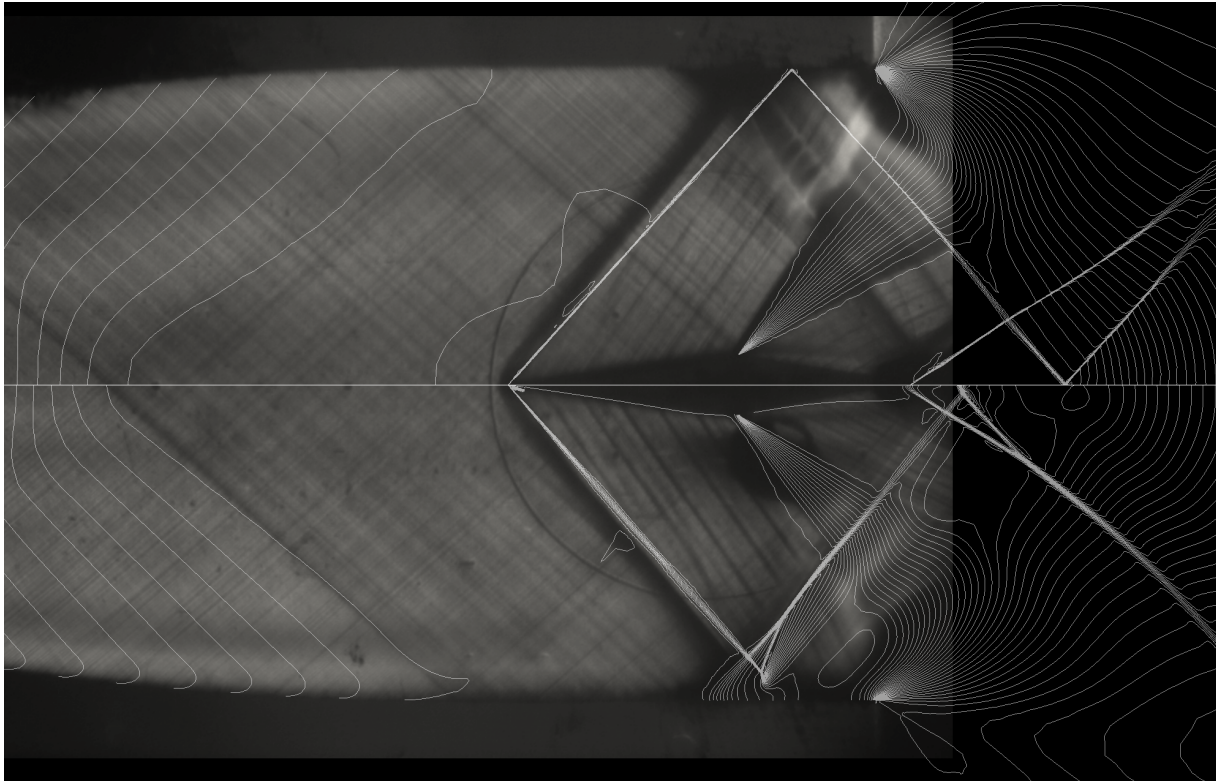
Discrepancies, with respect of experimental measurements, are found in the close proximity of the discharge section.

# Test case B: supersonic diamond-shaped airfoil



A mesh adaptation tool, developed at Politecnico di Milano, was coupled to SU2 to improve the quality of the grid in high gradient-regions and preserve a reasonable computational cost.

# Test case B: supersonic diamond-shaped airfoil



Euler (inviscid)

RANS (viscous)  
Spalart-Allmaras

The numerical solution includes a shock pattern that matches the one revealed by the experimental schlieren image.

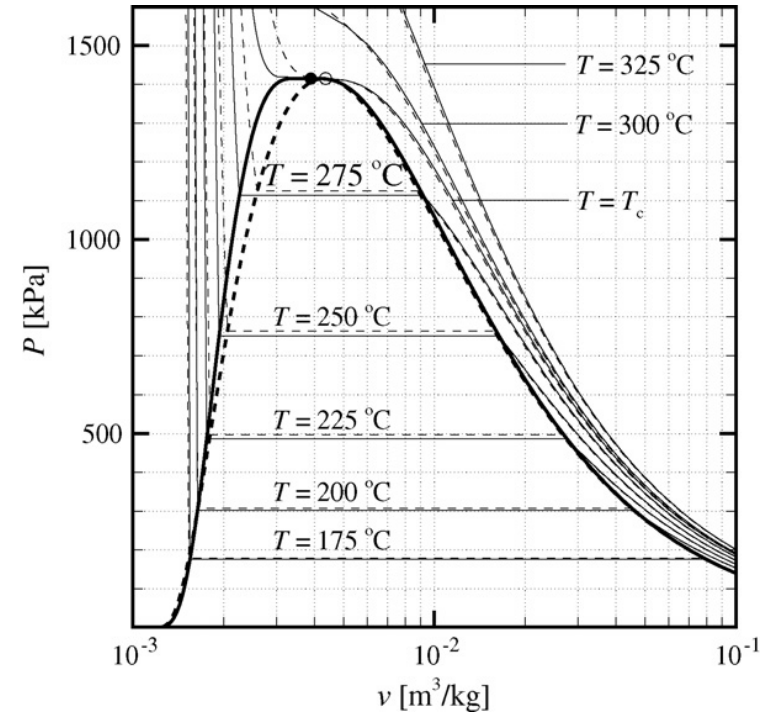
# Thermodynamics models... $PV \neq RT!$

$$\frac{\Psi(T, \rho)}{RT} = \psi^0(\tau, \delta) + \psi^r(\tau, \delta)$$

- Span-Wagner 12-parameter EoS (2003)

$$\begin{aligned} \psi^0(\tau, \delta) = & \frac{h_0^0 \tau}{RT_c} - \frac{s_0^0}{R} - 1 + \ln \left( \frac{\tau_0 \delta}{\delta_0 \tau} \right) \\ & - \frac{\tau}{R} \int_{\tau_0}^{\tau} \frac{C_P^0}{\tau^2} d\tau + \frac{1}{R} \int_{\tau_0}^{\tau} \frac{C_P^0}{\tau} d\tau \end{aligned}$$

$$\begin{aligned} \psi^r(\tau, \delta) = & n_1 \delta \tau^{0.250} + n_2 \delta \tau^{1.125} + n_3 \delta \tau^{1.500} + n_4 \delta^2 \tau^{1.375} \\ & + n_5 \delta^3 \tau^{0.250} + n_6 \delta^7 \tau^{0.875} + n_7 \delta^2 \tau^{0.625} e^{-\delta} \\ & + n_8 \delta^5 \tau^{1.750} e^{-\delta} + n_9 \delta \tau^{3.625} e^{-\delta^2} + n_{10} \delta^4 \tau^{3.625} e^{-\delta^2} \\ & + n_{11} \delta^3 \tau^{14.5} e^{-\delta^3} + n_{12} \delta^4 \tau^{12.0} e^{-\delta^3} \end{aligned}$$



$$P = P(E, \rho)$$



# Rules of the game: the governing equations

Euler equation for mono-component fluid at chemical and thermodynamic equilibrium

$$\left\{ \begin{array}{l} \partial_t \rho + \nabla \cdot (\rho \mathbf{u}) = 0, \\ \partial_t (\rho \mathbf{u}) + \nabla \cdot (\rho \mathbf{u} \otimes \mathbf{u} + P) = 0, \\ \partial_t E^t + \nabla \cdot [(E^t + P) \mathbf{u}] = 0, \end{array} \right. \quad \text{with} \quad E^t = \rho e + \frac{1}{2} \rho |\mathbf{u}|^2$$

Thermodynamic closure is needed!

Perfect gas:  $P = P(E, \rho) = (\gamma - 1) \rho e = (\gamma - 1) E$

# Thermodynamics models... $PV \neq RT!$

$$\frac{\Psi(T, \rho)}{RT} = \psi^0(\tau, \delta) + \psi^r(\tau, \delta)$$

## Span-Wagner 12-parameter EoS (2003)

$$\begin{aligned} \psi^r(\tau, \delta) = & n_1 \delta \tau^{0.250} + n_2 \delta \tau^{1.125} + n_3 \delta \tau^{1.500} + n_4 \delta^2 \tau^{1.375} + n_5 \delta^3 \tau^{0.250} + n_6 \delta^7 \tau^{0.875} + n_7 \delta^2 \tau^{0.625} e^{-\delta} \\ & + n_8 \delta^5 \tau^{1.750} e^{-\delta} + n_9 \delta \tau^{3.625} e^{-\delta^2} + n_{10} \delta^4 \tau^{3.625} e^{-\delta^2} + n_{11} \delta^3 \tau^{14.5} e^{-\delta^3} + n_{12} \delta^4 \tau^{12.0} e^{-\delta^3}, \end{aligned}$$

## Structure of the code changes deeply:

- Flux Jacobian is possibly NOT an homogeneous function of degree one w.r.t. conservative variables
- More complex eigenstructure w.r.t. ideal gas.
- Thermodynamics:
  - Computationally expensive
  - Possibly numerically unstable
  - Non-unique solutions (VLE)
  - $e \neq e(T)$ ,  $h \neq h(T)$ ,  $c \neq c(T)$
- Boundary conditions



# Rules of the game: the governing equations

Euler equation for mono-component fluid at chemical and thermodynamic equilibrium

$$\left\{ \begin{array}{l} \partial_t \rho + \nabla \cdot (\rho \mathbf{u}) = 0, \\ \partial_t (\rho \mathbf{u}) + \nabla \cdot (\rho \mathbf{u} \otimes \mathbf{u} + P) = 0, \\ \partial_t E^t + \nabla \cdot [(E^t + P) \mathbf{u}] = 0, \end{array} \right. \quad \text{with} \quad E^t = \rho e + \frac{1}{2} \rho |\mathbf{u}|^2$$

Thermodynamic closure is needed!

Perfect gas:  $P = P(E, \rho) = (\gamma - 1) \rho e = (\gamma - 1) E$

$$\frac{\Psi(T, \rho)}{RT} = \psi^0(\tau, \delta) + \psi^r(\tau, \delta)$$

Span-Wagner 12-parameter EoS (2003)

$$\begin{aligned} \psi^r(\tau, \delta) = & n_1 \delta \tau^{0.250} + n_2 \delta \tau^{1.125} + n_3 \delta \tau^{1.500} + n_4 \delta^2 \tau^{1.375} + n_5 \delta^3 \tau^{0.250} + n_6 \delta^7 \tau^{0.875} + n_7 \delta^2 \tau^{0.625} e^{-\delta} \\ & + n_8 \delta^5 \tau^{1.750} e^{-\delta} + n_9 \delta \tau^{3.625} e^{-\delta^2} + n_{10} \delta^4 \tau^{3.625} e^{-\delta^2} + n_{11} \delta^3 \tau^{14.5} e^{-\delta^3} + n_{12} \delta^4 \tau^{12.0} e^{-\delta^3}, \end{aligned}$$



# There may be trouble ahead...

## Structure of the code changes deeply:

- Flux Jacobian is possibly NOT an homogeneous function of degree one w.r.t. conservative variables (Roe scheme?)
- More complex eigenstructure w.r.t. ideal gas.
- Thermodynamics:
  - Computationally expensive
  - Possibly numerically unstable
  - Non-unique solutions (VLE)
  - Look-Up Table must be consistent
  - $e \neq e(T)$ ,  $h \neq h(T)$ ,  $c \neq c(T)$
- Boundary conditions

**...let's face the music and dance!**

